

¹ Context-dependent consequences of lagged effects in
² demographic models

³ Eric R. Scott¹, María Uriarte¹, Emilio M. Bruna¹

⁴ ¹Department of Wildlife Ecology and Conservation, University of Florida, Gainesville,
⁵ Florida 32611-0430 USA

⁶ ²Department of Ecology, Evolution and Environmental Biology, Columbia University 1200
⁷ Amsterdam Avenue, New York, New York 10027 USA

⁸ ³Center for Latin American Studies, University of Florida, Gainesville, Florida 32611-5530
⁹ USA

¹⁰ ⁴Biological Dynamics of Forest Fragments Project, INPA-PDBFF, CP 478, Manaus,
¹¹ Amazonas 69011-970 Brazil

¹² (draft: 23 April 2025)

¹³

Abstract

¹⁴ Text of 150 words max summarizing this amazing paper.

¹⁵ **Keywords:** demography, environmental stochasticity, integral projection models, lagged
¹⁶ effects, structured population models, population dynamics

¹⁷ **Manuscript elements:** Figure~1, figure~2, table~1, appendix~A..

¹⁸ **Manuscript type:** e-note

Introduction

20 There is increasing evidence that an organism's current likelihood of growth, survival,
 21 or reproduction can be strongly influenced by previous environmental conditions. These
 22 *Lagged Effects*, also known as *Delayed Life-history Events* (i.e., DLHEs) (Beckerman et
 23 al. 2002), can simultaneously affect an entire cohort (e.g., juveniles hatching during a
 24 period of scarcity will all have delayed maturation and lower lifetime fecundity) or only
 25 a subset of the population (e.g., cold temperatures in one year lead to reduced flowering
 26 by potentially reproductive individuals in the next). In addition, the temporal delay
 27 between an environmental event and changes in demographic vital rates depends on both
 28 the intensity of the event and its timing relative to the underlying physiological processes
 29 (Criley and Lekawatana 1994; Evers et al. 2021). A drought during the early stages of
 30 gestation or floral bud formation, for example, might have a much larger impact on the
 31 number of fruits or offspring produced than one several months later whose timing coincides
 32 with birth or flowering. The delay or intensity of lagged effects can also depend on local
 33 ecological conditions, with individuals in some habitats buffered against – or able to recover
 34 more quickly from - the delayed effects of environmental variation.

35

36 Because Lagged Effects are often directly linked to reproduction and survival, it is thought
 37 they could have major consequences for population dynamics (Beckerman et al. 2002).
 38 Although there is emerging evidence that this is indeed the case (Williams et al. 2015;
 39 e.g., Molowny-Horas et al. 2017; Tenhumberg et al. 2018), broader efforts to test this
 40 hypothesis have been hampered by two primary factors: First, detecting lagged effects
 41 requires long-term data on both the putative lagged effect (i.e., probability of flowering)
 42 and its potential environmental drivers (Metcalf et al. 2015). These coupled data sets
 43 are rare (*sensu* Evers et al. 2021), in part because studies to disentangle lagged effects
 44 can be challenging to design and maintain (Kuss et al. 2008). Second, the methods for
 45 identifying lagged effects and modeling their demographic impacts can be challenging to
 46 implement. Many of the statistical methods have stringent data requirements (Metcalf
 47 et al. 2015) and assumptions, while the including complex biological processes in demo-
 48 graphic models can render them less tractable. Addressing these obstacles is a major
 49 undertaking; the value of doing so will depend on the effort required vs. the potential
 50 consequences of failing to consider lagged effects - consequences that range from overesti-
 51 mating projections of population growth rate (i.e., λ) in a conservation setting to drawing
 52 invalid conclusions regarding support for the predictions of ecological or evolutionary theory.

53

54 Integral Projection Models (i.e., IPMs) are an important and widely used tool for studying
 55 demography and population dynamics (Ellner and Rees 2006; Rees and Ellner 2009; Rees
 56 et al. 2014). Their flexibility, in concert with a rapidly growing suite of software, data, and
 57 other resources (Salguero-Gómez et al. 2015; Ellner et al. 2016; Levin et al. 2021), have
 58 facilitated their use to study a wide range of topics in ecology, evolution, and conservation
 59 Crone et al. (2011). Mathematical and statistical advances (e.g., Williams et al. 2012;
 60 Brooks et al. 2019) have rapidly expand the scope of questions and biological processes that
 61 can be investigated with these models (e.g., Metcalf et al. 2015; Ellner et al. 2016; Rees
 62 and Ellner 2016). Here we investigate how including lagged effects in Integral Projection

63 Models influences projections of λ and population structure.

64

65 We have previously shown that the effects of precipitation extremes on the demographic
66 vital rates of an Amazonian understory herb (*Heliconia acuminata*, Heliconiaceae) can
67 be delayed up to 36 months (Scott et al. 2022), with the presence and duration of these
68 lagged effects varying by vital rate and habitat. We parameterized three classes of Integral
69 Projection Models - a deterministic IPM, a stochastic IPM, and a stochastic IPM with
70 lagged effects of precipitation on vital rates - for populations in two habitat type (i.e.,
71 continuous forest vs. forest fragments). Based on previous studies (Bruna et al. 2002; Bruna
72 and Kress 2002; Bruna 2003; Bruna and Oli 2005) and demographic theory (Tuljapurkar
73 1990; Caswell 2001) we predicted that: (i) projections of λ from deterministic models would
74 be higher than those of stochastic models, and that (ii) for all IPMs the projections of λ
75 forest fragments would be lower than for continuous forest, but that the difference would
76 be proportionately greater for IPM with lagged effects.

77

78

Methods

79 *Study System and Demographic Data*

80 *Heliconia acuminata* (Heliconiaceae) is a perennial, self-incompatible monocot that is
81 distributed throughout much of the Amazon basin (Kress 1990). While some *Heliconia*
82 species grow in large aggregations on roadsides, gaps, and in other disturbed habitats,
83 others - including *H. acuminata* - grow primarily in the forest understory (Kress 1983;
84 Ribeiro et al. 2010). Understory *Heliconia* species produce fewer flowers and are pollinated
85 by traplining hummingbirds (Stouffer and Bierregaard 1996; Bruna et al. 2004). The
86 models and analyses here are based on 11 years (1998-2009) of demographic data collected
87 on >8500 *H. acuminata* found at Brazil's Biological Dynamics of Forest Fragments Project
88 (BDFFP), located ~70 km north of Manaus, Brazil. The BDFFP reserves include both
89 continuous forest and forest fragments that range in size from 1-100 ha. These fragment
90 reserves were originally isolated in the early 1980's by the creation of cattle pastures, with
91 the secondary growth surrounding them periodically cleared to ensure their continued
92 isolation. The habitat in all sites is non-flooded lowland rain forest with rugged topography.
93 A complete summary of the BDFFP and its history can be found in Bierregaard et al. (2001).

94

95 A complete description of the demographic methods, data, and analyses to date can be
96 found in Bruna et al. (2023). Briefly, in 1997–1998 a series of 5000 m² plots were established
97 in the BDFFP reserves: N=6 in Continuous Forest and N=4 in 1-ha Forest Fragments.
98 All of the *Heliconia acuminata* in these plots were marked and measured; the plots were
99 censused annually, at which time a team recorded the size of surviving individuals, marked
100 and measured new seedlings, and identified any previously marked plants that died. Each
101 plot was also surveyed 4-5 times during the flowering season to identify reproductive plants;
102 in our site *H. acuminata* begin flowering early in the rainy season (e.g., January) and most
103 reproductive plants produce a single inflorescence (range = 1–7) with 20–25 flowers (Bruna
104 and Kress 2002). Fruits mature April-May and have 1–3 seeds per fruit ($\bar{x} = 2$) that are

105 dispersed by a thrush and several species of manakin (Uriarte et al. 2011). Dispersed seeds
 106 germinate approximately 6 months after dispersal at the onset of the subsequent rainy season,
 107 with rates of germination and seedling establishment higher in continuous forest than forest
 108 fragments (Bruna 1999; Bruna and Kress 2002). On average plots in CF also had more than
 109 twice as many plants as the plots in 1-ha fragments (CF median = 788, range = (201-1549);
 110 1-ha median = 339, range = (297-400)).

111 *Construction of Integral Projection Models*

112 We projected the growth rate and structure of *Heliconia acuminata* populations in Conti-
 113 nuous Forest and Forest Fragments with three classes of IPMs - Deterministic, Stochastic,
 114 and Stochastic with Lagged Environmental Effects. Each of these IPMs required different
 115 functional forms of the underlying vital rate functions used to describe the *H. acuminata*
 116 life cycle (Figure 1). All models were density-independent, with the deterministic model
 117 serving as the foundation for the more complex models.

118

119 **(1) Deterministic IPM:** In this model the size and structure of a population in year $t + 1$
 120 is determined by the survival and growth of plants alive in year t (Equation 1) plus the
 121 number of new seedlings that entered the population (Equation 2).

$$n(z', t + 1) = R(z')n_s(t) + \int_L^U P(z', z)n(z, t) dz \quad (1)$$

$$n_s(t + 1) = \int_L^U F(z)n(z, t) dz \quad (2)$$

122 Equation 1 has two components. The first is the sub-kernel $P(z', z)$, which describes the
 123 size-dependent survival and growth/regression of mature plants (Equation 3):

$$P(z', z) = s(z)G(z', z) \quad (3)$$

124 The second is sub-kernel $R(z')$, which describes the survival of seedlings established in year
 125 t and their size when entering the mature plant population in year $t + 1$ (Equation 4):

$$R(z') = s_s G_s(z') \quad (4)$$

126 Note that in Equation 4 both the probability that new seedlings survive their first year,
 127 s_s , and their size at the end of this year, $G(z', z)$, are size-independent. IPMs can include
 128 transitions between individuals from a discrete state to a continuous one (i.e., from ‘seedling’
 129 to ‘mature plant of size z' ,’ Ellner et al. 2016); we treat seedlings as a distinct and discrete
 130 category because they have lower survival and growth in their first year than comparably
 131 sized plants (Bruna 2003; Scott et al. 2022).

132

133 The number of new seedlings entering the population in year $t + 1$ is a function of the number
 134 of mature plants in year t and a sub-kernel describing the size-dependent fecundity of these
 135 individuals (Equation 5):

$$F(z) = p_f(z)f(z)g \quad (5)$$

136 Both the probability that a mature plant will flower, $p_f(z)$, and the number of seeds a
137 flowering plant will produce, $f(z)$, are size-dependent. All seeds germinate and establish as
138 seedlings with probability g .

139

140 We used the annual census data (Bruna 2003) to fit the deterministic vital rate functions
141 for growth, survival, and flowering in each habitat type (i.e., Fragments, Continuous Forest;
142 the data from all plots within a habitat class were pooled to create a single ‘summary
143 population’ (Bruna 2003). For established plants these were modeled as a smooth function
144 of size in the previous census with generalized additive models (GAMs) fit with the `mgcv`
145 library (Wood 2011) for the R statistical programming language (R Core Team 2020). For
146 consistency, seedling survival and growth were also modeled using GAMs, but without size
147 in the previous census as a predictor (i.e. ‘intercept-only’ models). For growth models a
148 scaled t family distribution provided a better fit to the data than a Gaussian fit, as the
149 residuals with a simple Gaussian model were Leptokurtic. To model size-specific fecundity
150 we used data on the number of fruits per flowering plant (Bruna 2021) and seeds per
151 fruit (Bruna 2014) that were collected outside of the demographic plots (to avoid altering
152 within-plot recruitment) and experimentally-derived estimates of seed germination and
153 seedling establishment (Bruna 1999, 2002).

154

155 **(2) Stochastic IPMs:** To include temporal stochasticity in our IPMs we included a
156 random effect of year. This was done using a factor-smooth interaction that allowed
157 the functional form of the relationship between plant size and vital rates to vary among
158 transition years (Figure 1). We generated kernels for every transition year using the
159 long-term survey data (Bruna et al. 2023) and random smooths for year. We then randomly
160 selected one of these sets of kernels to use in each iteration of the IPM. This procedure is
161 equivalent to ‘*kernel resampling*’ (*sensu* Metcalf et al. 2015) or matrix selection for matrix
162 population models (Caswell 2001).

163

164 **(3) Stochastic IPMs with lagged effects of precipitation on vital rates:** We explicitly
165 modeled the lagged effects of precipitation extremes on vital rates using the procedure
166 described in Scott et al. (2022). Briefly, we first calculated the Standardized Precipitation
167 Evapotranspiration Index (i.e., SPEI) for our study site using a published gridded dataset
168 based on ground measurements (Xavier et al. 2016). After we fit vital rate models using
169 the long-term survey data (Figure 1), we modeled delayed effects of SPEI with Distributed
170 Lag Non-linear Models (i.e., DLNMs) with a maximum lag of 36 months (Scott et al. 2022).
171 To iterate these parameter-resampled IPMs (*sensu* Metcalf et al. 2015) we first created a
172 random sequence of SPEI values by sampling years of the observed (monthly) SPEI data.
173 For every year we then calculated a lag of 36 months from the month in which that year’s
174 census was completed. These values were then used to predict the fitted values from vital
175 rate models, which generated different kernels for each iteration of the IPM. The kernels of
176 successive iterations are not entirely independent – the SPEI values used to calculate vital
177 rates include values used in the previous two iterations – they are ergodic.

178

179 All IPMs were constructed and iterated using the `ipmr` package (Levin et al. 2021) for the

180 R statistical programming language (R Core Team 2020). The IPMs used 100 meshpoints
181 and the midpoint rule for calculating kernels . For each type of IPM we iterated the
182 model for 1000 time steps, but discarded the first 100 time steps to omit transient effects.
183 Stochastic growth rates (λ_s) were calculated as the average $\ln(\lambda)$ from each time step
184 (Caswell 2001) and then back-transformed to allow for direct comparison with projections of
185 λ from deterministic models. The initial starting vector primarily influences a population's
186 transient dynamics; we therefore used the distribution of established plant sizes and
187 proportion of seedlings in the full demographic data set as the initial population vector for
188 all models. Finally, we estimated the 95% confidence intervals for each IPMs projections of
189 λ . To do so we first created 500 populations for each habitat type by sampling individual
190 plants with replacement (i.e., bootstrapping) until the population size of each matched
191 that of the initial population vector. We then re-fit the vital rate models for growth,
192 survival, and flowering for each of these bootstrapped population and constructed new
193 IPMs for each population as above (the models for germination and establishment rate,
194 fruits per flowering plant, and seeds per fruit were not refit because these were estimated
195 using different data sets). The projections of λ for the new populations were then used to
196 estimate the upper and lower 95% bias-corrected percentile intervals (Caswell 2001; Manly
197 2018). This workflow was managed using the **targets** R package (Landau 2021), which
198 also allowed us to track computational time spent processing and analyzing each class of IPM.

199

200 **Statistical analyses**

201 **Comparison of CF vs FF**

- 202 • For det need to bootstrap
- 203 • for within stoch and lag: glm/t-test.
- 204 • Comparison of pop structure in figure (test for increasing variance with variance /
205 F or permutation test). Villase nor, J. A., & González-Estrada, E. (2024). A non-
206 parametric test for homogeneity of variances. Communications in Statistics - Theory
207 and Methods, 54(2), 646–654. <https://doi.org/10.1080/03610926.2024.2316274>
208 OR https://www.datanovia.com/en/lessons/homogeneity-of-variance-test-in-r/#google_vignette

210

Results & Discussion

211 **Lambda Comparison**

- 212 1. We found that including Delayed Life-History Events in Intergral Projection Models
213 led to significantly lower projections of λ
- 214 2. It is reassuring that all IPM models projected higher values of λ in continuous forest
215 than forest fragments (Table 2); this is consistent with the results of previous studies
216 comparing the relative rankings of projections from stochastic and deterministic models
217 (e.g., Kaye and Pyke 2003.)
- 218 3. However, the underestimating λ by 2-3% difference in λ resulting projections from the
219 different IPMs could have major implications for many of the contexts in which IPMs

- 220 are brought to bear.
221 4. If you are doing conservation and management, a growth rate lower by 5-6 % would
222 really rock your world.
223 5. For instance, underestimating λ by failing to include lagged effects could be especially
224 severe in studies of climate change, given many DLHE are climate driven.

225

226 **Pop Structure Comparison**

- 227 1. Including lagged effects in IPMs also resulted in more variable projections of future
228 population structure (Figure 2 a), especially in forest fragments where we have previously
229 shown lagged effects have very large impacts on growth and survival (Scott et al.
230 2022).
231 2. Consequently, projections of population structure were also far less consistent
232 across habitats (Figure 2 b).
233 3. Finally, the choice of IPM also resulted in some subtle but notable differences in
234 projected population structure.
235 4. For example, the deterministic IPM projected the population in Continuous Forest
236 had slightly more of the smallest and largest plants than the population in Forest
237 Fragments.
238 5. In other words, populations in forest fragments had proportionately less recruitment
239 and fewer individuals growing into the larger and reproductive size classes (Bruna
240 and Oli 2005).
241 6. The shift towards intermediately sized, pre-reproductive plants in forest fragments is
242 even more dramatic when using the parameter-resampled stochastic IPM (Figure 2
243 b).
244

245 **So...should we care?**

- 246 1. Including delayed life-history events in demographic models has important implications
247 both projections of population growth rate and population structure.
248 2. These projections may be more accurate - the underlying vital rate models for IPMS
249 with Lagged effects all had the best fit to the survey data ($dAIC = 0$, Table 1).
250 3. While this may not be critical in situations where relative differences allow for hypothesis
251 testing, it may be especially important in conservation or management settings.
252 4. Including lagged effects comes at a cost, however.
253 5. While Deterministic and Kernel-resampled Stochastic IPMs took only ~ 0.02 and ~ 0.07
254 min to iterate (respectively), the Stochastic IPMs with using parameter-resampled
255 kernels and lagged effects took ~ 87.12 min.
256 6. This is largely due to the required computational resources and algorithms (i.e.,
257 `predict()`), which are much slower for General Additive Models (i.e., GAMs) with
258 2D smooths because of the much higher number of knots than for the GAMs used in
259 Deterministic and Kernel-resampled IPMs.
260 7. Advances in computational power and access to high-performance computing resources

261 could lower this cost.

- 262
- 263 8. However, computational power cannot compensate for limited data.
- 264 9. Detecting lagged effects and evaluating their consequences requires long-term demo-
- 265 graphic data - data that are only available for a relatively small number of species, few
- 266 of which are in the tropics.
- 267 10. The increasing evidence that lagged effects are ubiquitous, and that they can have
- 268 major demographic impacts, underscores the need to support the collection of such
- 269 long-term data, the complementary development of experimental and statistical
- 270 approaches to disentangling lagged effects, and community driven efforts to identify
- 271 priority or model systems for in-depth investigation.
- 272

273 Acknowledgments

274 We thank _____, _____, and _____ anonymous reviewers for helpful discussions and comments
275 on the manuscript. We also thank Sam Levin for his help with the `ipmr` package. Fi-
276 nancial support for collecting the demographic data used in this study was provided by the
277 U.S. National Science Foundation (awards INT 98-06351, DEB-0309819, DEB-0614149,DEB-
278 0614339, and DEB-1948607). This article is publication no. _____ in the BDFFP Technical
279 series. The authors declare no conflicts of interest.

280 CRediT Statement

281 ERS contributed to the conceptualization, methodology, formal analysis, and led the writing
282 of the original draft. EMB contributed to the conceptualization, methodology, writing, and,
283 acquired funding.

284 Data Availability Statement

285 Data and R code used in this study are archived with Zenodo at (*doi and url to be added on*
286 *acceptance*).

287

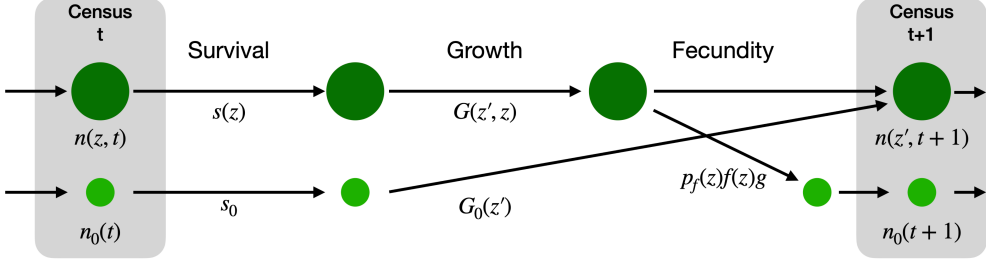
Literature Cited

- 288 Beckerman, A., T. G. Benton, E. Ranta, V. Kaitala, and P. Lundberg. 2002. [Population](#)
289 [dynamic consequences of delayed life-history effects](#). Trends in Ecology & Evolution 17:263–
290 269.
- 291 Bierregaard, R. O., C. Gascon, T. E. Lovejoy, and R. Mesquita, eds. 2001. Lessons from
292 Amazonia: The ecology and conservation of a fragmented forest. Yale University Press, New
293 Haven.
- 294 Brooks, M. E., K. Kristensen, M. R. Darrigo, P. Rubim, M. Uriarte, E. Bruna, and B. M.
295 [Bolker](#). 2019. [Statistical modeling of patterns in annual reproductive rates](#). Ecology 100.
- 296 Bruna, E. M. 1999. [Seed germination in rainforest fragments](#). Nature 402:139.
- 297 ———. 2002. [Effects of forest fragmentation on *Heliconia acuminata* seedling recruitment in central Amazonia](#). Oecologia 132:235–243.
- 299 Bruna, E. M. 2003. [Are plant populations in fragmented habitats recruitment limited? Tests with an Amazonian herb](#). Ecology 84:932–947.
- 301 ———. 2014. [Dataset: *Heliconia acuminata* seed set \(seeds per fruit\)](#). Figshare doi: 10.6084/m9.figshare.1273926.v2.
- 303 ———. 2021. [Dataset: Leaf number, leaf area, shoot number, and height of reproductive H. acuminata](#). Zenodo <https://doi.org/10.5281/zenodo.5041931>.
- 305 Bruna, E. M., and W. J. Kress. 2002. [Habitat fragmentation and the demographic structure of an Amazonian understory herb \(*Heliconia acuminata*\)](#). Conservation Biology 16:1256–1266.
- 308 Bruna, E. M., W. J. Kress, F. Marques, and O. F. da Silva. 2004. [Heliconia acuminata reproductive success is independent of local floral density](#). Acta Amazonica 34:467–471.
- 310 Bruna, E. M., O. Nardy, S. Y. Strauss, and S. Harrison. 2002. [Experimental assessment of *Heliconia acuminata* growth in a fragmented Amazonian landscape](#). Journal of Ecology 90:639–649.
- 313 Bruna, E. M., and M. K. Oli. 2005. [Demographic Effects of Habitat Fragmentation on a Tropical Herb: Life-Table Response Experiments](#). Ecology 86:1816–1824.
- 315 Bruna, E. M., M. Uriarte, M. R. Darrigo, P. Rubim, C. F. Jurinitz, E. R. Scott, O. Ferreira da Silva, et al. 2023. [Demography of the understory herb *Heliconia acuminata* \(Heliconiaceae\) in an experimentally fragmented tropical landscape](#). Ecology 104:e4174.

- 318 Caswell, H. 2001. Matrix population models: Construction, analysis, and interpretation.
319 Sinauer Associates, Sunderland.
- 320 Criley, R., and S. Lekawatana. 1994. Year around production with high yields may be
321 a possibility for *Heliconia chartacea*. Acta Horticulturae, New ornamental crops and the
322 market for floricultural products 397:95–102.
- 323 Crone, E. E., E. S. Menges, M. M. Ellis, T. Bell, P. Bierzychudek, J. Ehrlen, T. N. Kaye, et
324 al. 2011. How do plant ecologists use matrix population models? Ecology Letters 14:1–8.
- 325 Ellner, S. P., D. Z. Childs, and M. Rees. 2016. Data-driven modelling of structured popula-
326 tions: A practical guide to the integral projection model. Springer Science+Business Media,
327 New York, NY.
- 328 Ellner, S. P., and M. Rees. 2006. Integral projection models for species with complex
329 demography. American Naturalist 167:410–428.
- 330 Evers, S. M., T. M. Knight, D. W. Inouye, T. E. X. Miller, R. Salguero-Gómez, A. M. Iler,
331 and A. Compagnoni. 2021. Lagged and dormant season climate better predict plant vital
332 rates than climate during the growing season. Global Change Biology 27:1927–1941.
- 333 Kaye, T. N., and D. A. Pyke. 2003. The effect of stochastic technique on estimates of
334 population viability from transition matrix models. Ecology 84:1464–1476.
- 335 Kress, J. 1990. The diversity and distribution of *heliconia* (Heliconiaceae) in Brazil. Acta
336 Botanica Brasileira 4:159–167.
- 337 Kress, W. J. 1983. Self-incompatibility systems in Central American *heliconia*. Evolution
338 37:735–744.
- 339 Kuss, P., M. Rees, H. H. Ægisdóttir, S. P. Ellner, and J. Stöcklin. 2008. Evolutionary
340 demography of long-lived monocarpic perennials: A time-lagged integral projection model.
341 Journal of Ecology 96:821–832.
- 342 Landau, W. M. 2021. The targets R package: A dynamic Make-like function-oriented
343 pipeline toolkit for reproducibility and high-performance computing 6:2959.
- 344 Levin, S. C., D. Z. Childs, A. Compagnoni, S. Evers, T. M. Knight, and R. Salguero-Gómez.
345 2021. Ipmr: Flexible implementation of Integral Projection Models in R. Methods in Ecology
346 and Evolution 12:1826–1834.
- 347 Manly, B. F. 2018. Randomization, bootstrap and Monte Carlo methods in biology. chap-
348 man; hall/CRC.
- 349 Metcalf, C. J. E., S. P. Ellner, D. Z. Childs, R. Salguero-Gómez, C. Merow, S. M. McMahon,

- 350 E. Jongejans, et al. 2015. [Statistical modelling of annual variation for inference on stochastic](#)
351 [population dynamics using Integral Projection Models](#). Methods in Ecology and Evolution
352 6:1007–1017.
- 353 Molowny-Horas, R., M. L. Suarez, and F. Lloret. 2017. [Changes in the natural dynamics](#)
354 [of *Nothofagus dombeyi* forests: Population modeling with increasing drought frequencies](#).
355 Ecosphere 8:1–17.
- 356 Morris, W. F., and D. F. Doak. 2002. Quantitative conservation biology: Theory and
357 practice of population viability analysis. Sinauer, Sunderland, MA.
- 358 R Core Team. 2020. *R: A language and environment for statistical computing*. Vienna,
359 Austria.
- 360 Rees, M., D. Z. Childs, and S. P. Ellner. 2014. [Building integral projection models: A user’s](#)
361 [guide](#). Journal of Animal Ecology 83:528–545.
- 362 Rees, M., and S. P. Ellner. 2009. [Integral projection models for populations in temporally](#)
363 [varying environments](#). Ecological Monographs 79:575–594.
- 364 ———. 2016. [Evolving integral projection models: Evolutionary demography meets eco-](#)
365 [evolutionary dynamics](#). Methods in Ecology and Evolution 7:157–170.
- 366 Ribeiro, M. B. N., E. M. Bruna, and W. Mantovani. 2010. [Influence of post-clearing](#)
367 [treatment on the recovery of herbaceous plant communities in Amazonian secondary forests](#).
368 Restoration Ecology 18:50–58.
- 369 Salguero-Gómez, R., O. R. Jones, C. R. Archer, Y. M. Buckley, J. Che-Castaldo, H. Caswell,
370 D. Hodgson, et al. 2015. [The COMPADRE Plant Matrix Database: An open online reposi-](#)
371 [tory for plant demography](#). (M. Rees, ed.)Journal of Ecology 103:202–218.
- 372 Scott, E. R., M. Uriarte, and E. M. Bruna. 2022. [Delayed effects of climate on vital rates](#)
373 [lead to demographic divergence in Amazonian forest fragments](#). Global Change Biology
374 28:463–479.
- 375 Stouffer, P. C., and R. O. Bierregaard. 1996. Forest fragmentation and seasonal patterns of
376 hummingbird abundance in Amazonian Brazil. Ararajuba 4:9–14.
- 377 Tenhumberg, B., E. E. Crone, S. Ramula, and A. J. Tyre. 2018. [Time-lagged effects of](#)
378 [weather on plant demography: Drought and *Astragalus scaphoides*](#). Ecology 99:915–925.
- 379 Tuljapurkar, S. 1990. [Population Dynamics in Variable Environments](#). (S. Levin, ed.)Lecture
380 Notes in Biomathematics (Vol. 85). Springer, Berlin, Heidelberg.
- 381 Uriarte, M., M. Anciães, M. T. B. da Silva, R. Rubim, E. Johnson, and E. M. Bruna. 2011.

- ³⁸² Disentangling the drivers of reduced long-distance seed dispersal by birds in an experimen-
³⁸³ tally fragmented landscape. *Ecology* 92:924–937.
- ³⁸⁴ Williams, J. L., H. Jacquemyn, B. M. Ochocki, R. Brys, T. E. X. Miller, and R. Sheffer-
³⁸⁵ son. 2015. Life history evolution under climate change and its influence on the population
³⁸⁶ dynamics of a long-lived plant. *Journal of Ecology* 103:798–808.
- ³⁸⁷ Williams, J. L., T. E. Miller, and S. P. Ellner. 2012. Avoiding unintentional eviction from
³⁸⁸ integral projection models. *Ecology* 93:2008–2014.
- ³⁸⁹ Wood, S. N. 2011. Fast stable restricted maximum likelihood and marginal likelihood esti-
³⁹⁰ mation of semiparametric generalized linear models 73:3–36.
- ³⁹¹ Xavier, A. C., C. W. King, and B. R. Scanlon. 2016. Daily gridded meteorological variables
³⁹² in Brazil (1980–2013). *International Journal of Climatology* 36:2644–2659.



Description	Deterministic	Stochastic, kernel-resampled	Stochastic, parameter-resampled
Survival	$s(z)$	$s_y(z)$	$s(z; \theta_{0-36})$
Growth	$G(z'; z)$	$G_y(z'; z)$	$G(z'; z; \theta_{0-36})$
Flowering	$p_f(z)$	$p_{f_y}(z)$	$p_f(z; \theta_{0-36})$
Size-specific fecundity	$f(z)$	$f(z)$	$f(z)$
Germination & establishment	g	g	g
Seedling survival	s_0	s_{0_y}	$s_0(\theta_{0-36})$
Seedling growth	$G_0(z')$	$G_{0_y}(z')$	$G_0(z'; \theta_{0-36})$

Figure 1: Life cycle diagram of *Heliconia acuminata*. Each transition is associated with an equation for a vital rate function. The functions shown on the diagram correspond to those used to construct a general, density-independent, deterministic IPM. The table below shows the equivalent equations for stochastic, kernel-resampled IPMs and stochastic, parameter-resampled IPMs.

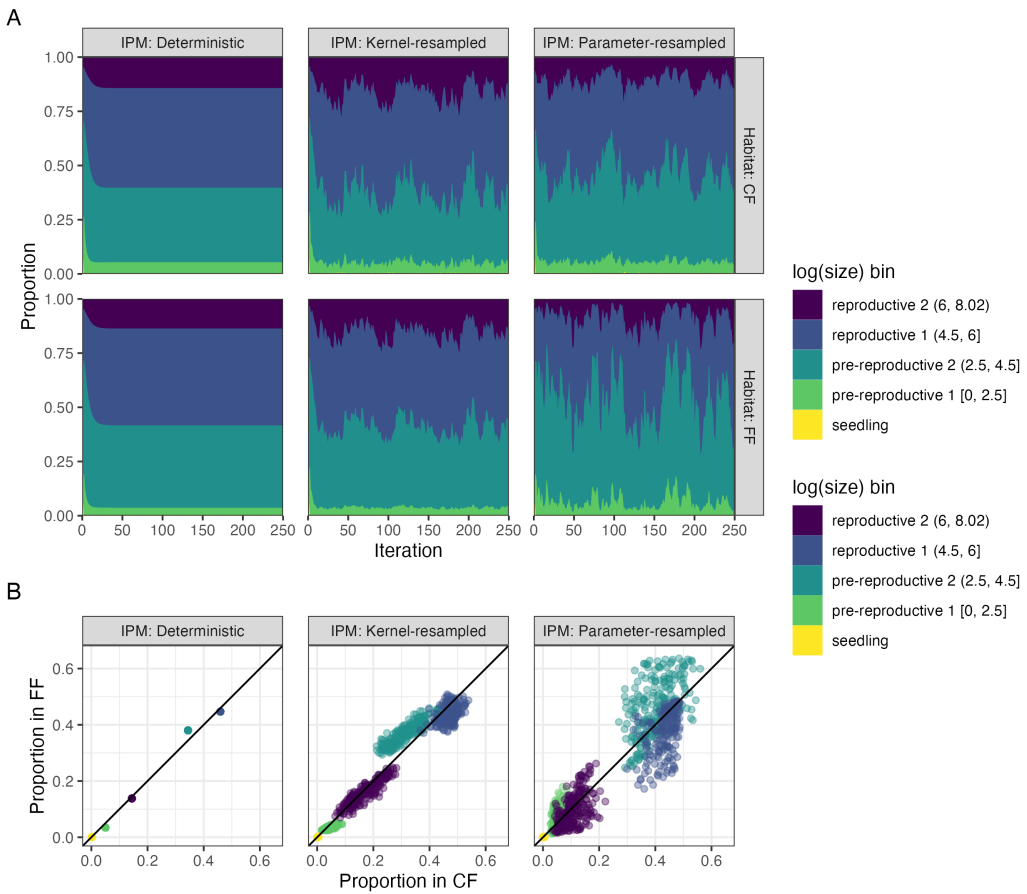


Figure 2: **(A)** The proportion of *Heliconia acuminata* populations in different size/stage classes when simulating population dynamics with three different Integral Projection Models. Results are shown for the first 250 iterations of populations in both in Continuous Forest (CF) and Forest Fragments (FF); for the criteria used to define the size categories see Table 3. **(B)** For each iteration, the relative proportion of the population in each size class (FF vs CF). Note that this excludes transient dynamics (iterations 1-30). Values on the 1-1 line indicate an iteration where CF and FF have the same proportion of the population in a given size class.

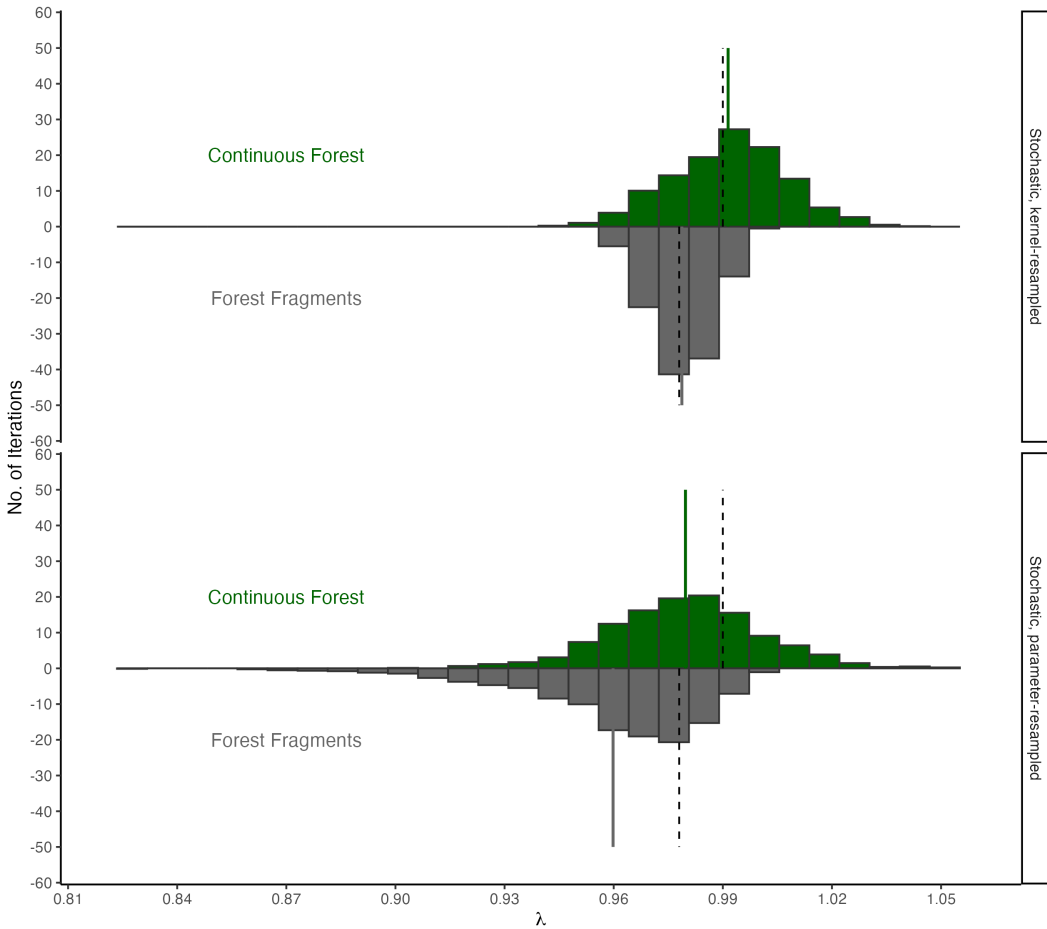


Figure 3: Distribution of 900 values of λ projected with (A) Stochastic, kernel-resampled IPMs and (B) Stochastic, parameter-resampled IPMs. IPMs were used to project λ for both Continuous Forest (green) and Forest Fragments (gray). The solid line indicates the mean value, the dashed line indicates the value of λ in that habitat projected with Deterministic IPMs.

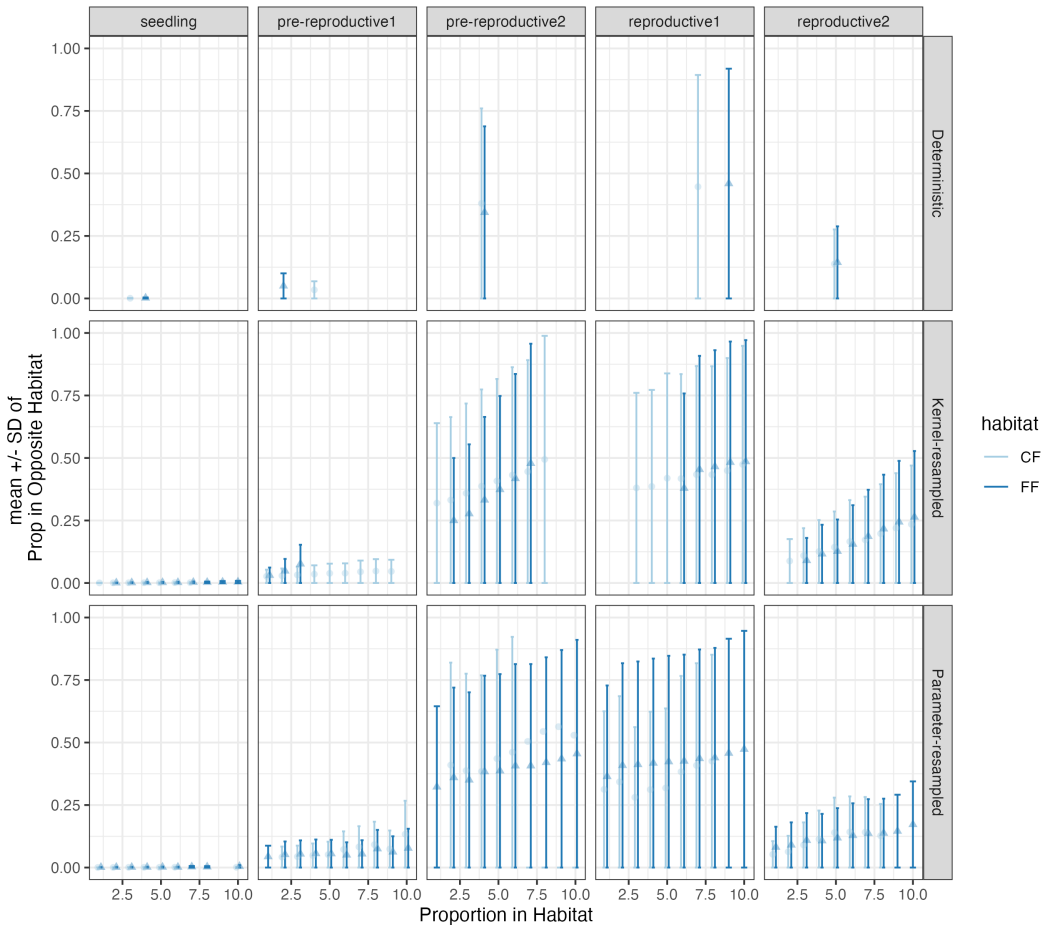


Figure 4: ——

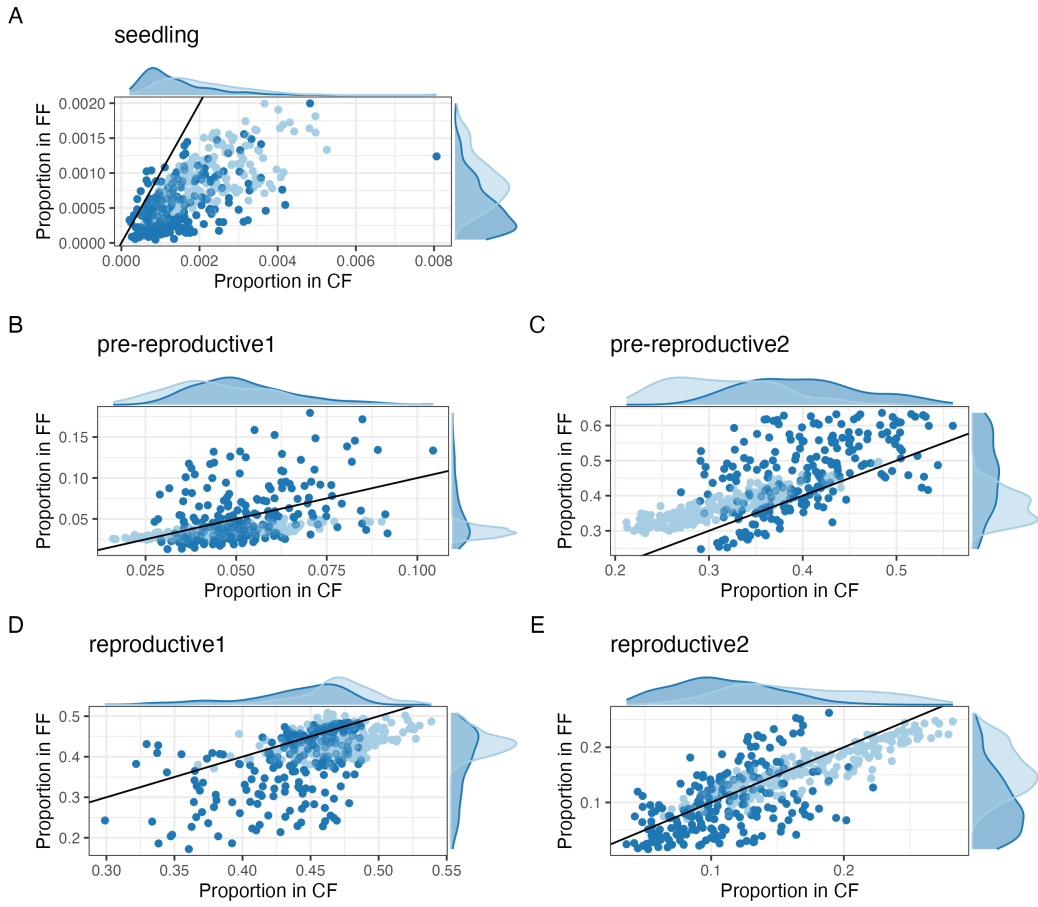


Figure 5: ——

Table 1: Comparison of vital rate models used to build IPM. The ‘Effect of Environment’ column describes how environmental effects were included in models. Those with ‘none’ were used to build deterministic IPMs; those with a random effect of year were used to build stochastic, kernel-resampled IPMs; and those with a distributed lag non-linear model (DLNM) were used to build stochastic, parameter-resampled IPMs. ‘edf’ is the estimated degrees of freedom of the penalized GAM. ΔAIC is calculated within each habitat and vital rate combination. ΔAIC within 2 indicates models are equivalent.

Habitat	Vital Rate	Effect of Environment	edf	ΔAIC
Continuous Forest				
	Survival	Random effect of year	43.26	0.00
		DLNM	19.72	78.92
		None	4.98	260.01
	Growth	Random effect of year	78.43	0.00
		DLNM	23.87	158.46
		None	7.81	1896.03
	Flowering	DLNM	19.59	0.00
		Random effect of year	17.19	1.63
		None	7.47	381.86
	Seedling survival	None	1.00	0.00
		Random effect of year	1.82	1.39
		DLNM	4.01	1.53
	Seedling growth	Random effect of year	9.47	0.00
		DLNM	8.95	2.90
		None	1.00	172.33
Forest Fragments				
	Survival	DLNM	14.95	0.00
		Random effect of year	19.21	35.68
		None	4.33	51.25
	Growth	DLNM	25.18	0.00
		Random effect of year	37.84	199.98
		None	5.60	382.76
	Flowering	DLNM	20.61	0.00
		Random effect of year	13.81	27.40
		None	5.01	101.70
	Seedling survival	DLNM	5.57	0.00
		Random effect of year	5.09	5.72
		None	1.00	6.49
	Seedling growth	Random effect of year	6.25	0.00
		DLNM	8.18	2.29
		None	1.00	5.74

Table 2: Population growth rates for continuous forest (CF) and forest fragments (FF) under different kinds of IPMs with bootstrapped, bias-corrected, 95% confidence intervals.

IPM	Habitat	λ
Deterministic		
	FF	0.9778 (0.9736, 0.9823)
	CF	0.9897 (0.9877, 0.9920)
Stochastic, kernel resampled		
	FF	0.9787 (0.9735, 0.9835)
	CF	0.9913 (0.9892, 0.9939)
Stochastic, parameter-resampled		
	FF	0.9595 (0.9459, 0.9689)
	CF	0.9795 (0.9752, 0.9867)

Table 3: Size and stage categories used for comparing *Heliconia acuminata* population structure. Note that seedlings are a discrete size class not based on size (see *Methods* for additional details).

category	log(size)	avg. prob. survival	prob. flowering
seedlings	-	-	-
pre-reproductive 1	0–2.5	≤ 0.9	≈ 0
pre-reproductive 2	2.5–4.5	≥ 0.8	≈ 0
reproductive 1	4.5–6	≥ 0.95	≤ 0.25
reproductive 2	≥ 6	≥ 0.95	≥ 0.2